Global detection and identification of components from *Yunnan Baiyao* based on Liquid Chromatography Hybrid Ion Trap Time-of-Flight Mass Spectrometry

Chen Dai[1], Yan Liang[1], Haiping Hao*, Xiao Zheng, Lin Xie, Tianye Guan, Yuanyuan Zhou, Guangji Wang**

State Key Lab of Natural Medicines, Key Lab of Drug Metabolism & Pharmacokinetics, China Pharmaceutical University, No. 24, Tongjia Lane, Nanjing 210009, China

[1] These authors contributed equally to this work.

** **Correspondence:** Professor Guangji Wang, State Key Lab of Natural Medicines, Key Lab of Drug Metabolism & Pharmacokinetics, China Pharmaceutical University, No. 24, Tongjia Lane, Nanjing 210009, China

Email: guangjiwang@hotmail.com **Fax:** +86-25-83302827

* Co- corresponding author: Professor Haiping Hao

Email: hhp_770505@yahoo.com.cn

Abbreviation: **Ara**, Arabinopyranosyl; **DFIs**, Diagnostic fragment ions; **Glc**, Glucopyranosyl; **TCMP**, Traditional Chinese medicine prescription; **Rha**, Rhamnopyranosyl; **Rt**, retention time; **Xyl**, Xylopyranosyl; **YNBY**, *Yunnan Baiyao*

Keywords: *Yunnan Baiyao* / diagnostic ion filtering / polarity directed extraction / Structural characterization

Received: March 2, 2013; Revised: March 16, 2013; Accepted: March 22, 2013

Abstract

Yunnan Baiyao is a widely used herbal prescription in traditional medicine for the treatment of bleeding and hematological diseases, while its chemical profile remains elusive. In this work, a novel methodology combining polarity directed extraction technique with a diagnostic ion filtering strategy based on liquid chromatography hybrid ion trap time-of-flight mass spectrometry analysis was developed for global, efficient and rapid characterization of components in *Yunnan Baiyao*. Di-ethyl ether, n-butanol and ethanol-water (70:30, v/v) covering low to high polarity ranges were chosen as the extraction solvent respectively. The results clearly showed that, compared with conventional single extraction solvent, collaboratively using extraction solvents with different polarity can effectively increase the number of detected peaks and enrich the product ions information in multistage mass spectra analysis. By further matching diagnostic ions and fragmental pathways, a total of 34 components were successfully identified. Our work clearly demonstrate that integrating polarity directed extraction and diagnostic ion filtering techniques is a powerful and reliable strategy for global detection and identification of complex chemicalome from herbal prescriptions, and may open new avenues for chemical analysis in other complex mixtures.

1 Introduction

Traditional Chinese medicine prescription (TCMP), the concoction of several single herbs, has been an essential part of the health care system in many oriental countries for thousands of years [1-4]. Over the past decades, TCMP has been one of the main resources for screening lead compounds in medicinal practice. To further facilitate the drug discovery efficiency from herbal medicine and explore the pharmacological mechanism of TCMP, unambiguous

detection and identification of active components in TCMP are the prerequisite step. Nevertheless, due to the inherent complexity of herbal prescription, the qualitative analysis of TCMP was acknowledged as a tremendous challenge which imposes restriction on the modernization of TCMP.

Recently, with the prevalence of hyphenated chromatographic approaches such as LC/MS and GC/MS, researchers can deduce the structure of phytochemical constituents in TCMP based on information obtained such as retention time, UV spectra and ion fragmentation behaviors [5-9]. Although the reference compounds are not always available, with the application of high resolution mass spectrum and multistage mass spectra (MS^n, $n\geq2$), e.g., the hybrid ion trap and time-of-flight mass spectrometry (LC/MS-IT-TOF) that integrates the merits of ion trap in producing multistage tandem ($MS^{1–10}$) fragmentations and TOF in high resolution and accurate mass measurement, researchers could tentatively infer the structure of unknown compounds in TCMP based on the accurate molecular weight and the relationship between precursor and daughter ions [10]. Admittedly, obtaining abundant mass spectrum information is a key step in the structural inference process. Generally, efficient sample preparation can enrich the target analytes and subsequently improve fragmental performance of analytes in mass instrument. The conventional sample preparation approach for TCMP was liquid-solid extraction. Specifically, researchers often utilize ultrasound assisted extraction process for TCMP using a mixed solvent system composed of ethanol/methanol and water at a certain volume ratio [11-15]. However, it is well known that the components contained in TCMP usually cover a large range of concentrations (over 10^3 orders of magnitude) and possess various physicochemical properties (e.g., polarity and solubility). Therefore, utilizing a single mixed solvent system for extraction of TCMP could miss some components whose physiochemical properties were far distinguished from the extraction solvent. Consequently, the mass spectrum obtained for the extracted sample will tend to generate limited peak

detection and inadequate fragment ions information, which presumably could create obstacles for a global qualitative analysis of TCMP.

To solve the problem, a polarity directed extraction strategy was developed for the purpose of obtaining abundant mass spectrum information. Such a strategy was proposed from the premise that a component with defined polarity will be adequately extracted into a solvent which has close polarity. Stronger mass spectrum response and potential more fragments ions could be obtained by using this strategy for sample preparation. Following this idea, a series of solvents with a polarity range from low to high could be applied with sonication to extract TCMP respectively, and then each extracted portion is subjected to LC/MS-IT-TOF for analysis. Subsequently, a diagnostic ion filtering method, which had been successfully applied to multi-components identification of TCMP, could be readily employed for rapid and reliable structural characterization based on sufficient fragment ions information generated [9, 16-18].

In the present work, *Yunnan Baiyao*, a well-known herb prescription used in oriental countries for more than 100 years for hemostasis and dispersing blood stasis, was used as an example to demonstrate how the strategy could be employed to facilitate optimal analytical performance for multi-components [19-20]. Notably, as a state-protected TCMP with Class-1 confidential prescription in China, the exact composition of *Yunnan Baiyao* remains unknown. To date, very little is known about its chemical constitutions [21]. Using the methodology presented here, we successfully detected and identified 34 components from Yunnan Baiyao.

2 Experimental

2.1 Reagents and Chemicals

Authentic standards of Notoginsenoside R_1, Ginsenoside Rg_1, Rf, Rh_1, F_1, and Ra_3 were purchased from the Department of Nature Medicinal Chemistry in Jilin University (Jilin,

China), and Dencichine, Parissaponin Pb were supplied by the Weikeqi biotechnology Co., Ltd. (Sichuan, China). *Yunnan Baiyao* powder (Batch No. 20080804C) was supplied by the *Yunnan Baiyao* Group Co., Ltd. (Kunming, Yunnan, China). HPLC-grade acetonitrile and methanol were purchased from Fisher Scientific (Fair Lawn, NJ, USA). Analytical-grade Di-Ethyl Ether, ethanol and n-butanol were purchased from Shanghai Shiyi Chemicals Reagent Co., Ltd. (Shanghai, China). Formic acid was of HPLC grade (Tedia, USA). Ultrapure water was prepared using a Milli-Q Ultrapure water purification system (Millipore, Bedford, MA, USA).

2.2 Sample preparation based on polarity directed extraction technique

The performance of a series of organic solvents including 50% ethanol, 70% ethanol, 70% n-butanol, n-butanol, ethyl acetate and di-ethyl ether, to extract the constituents from *Yunnan Baiyao*, was investigated. At the end, di-ethyl ether, n-butanol and ethanol-water (70:30), with a polarity range from low to high, were chosen as the extraction solvent since maximum components could be extracted by this system. Three portions of *Yunnan Baiyao* powder (50 mg of each) were respectively extracted by sonication (ultrasonic power: 100 W) with 10 mL di-Ethyl Ether, n-butanol and ethanol-water (70:30, v/v) for two cycles (1 h per cycle) at room temperature. The extracts derived from different extraction solvents were separately filtered through nylon 6,6 membrane filter (5 μm), each filtrate was condensed under reduced pressure using a rotary evaporator at 50℃. The residues were respectively reconstituted with 1 mL of methanol followed by centrifugation at 20,000 g for 10 min, and then each volume of 5 μL supernatant was injected into the LC-IT-TOF/MS for analysis.

2.3 LC/MS -IT-TOF parameters

All sample analysis was carried out on a LC/MS-IT-TOF system (Shimadzu, Tokyo, Japan). Chromatographic separation was achieved on a Luna^{TM} C_{18} column (5 μm, 150×2.00 mm I.D., Phenomenex) at 35℃. The mobile phase (delivered at 0.2 mL/min) composed of solvent A (0.02% formic acid in water, v/v) and B (100% acetonitrile, v/v). A binary gradient elution was performed: initially 20% B for 5 min, linear gradient 20-40% B from 5 to 40 min and 40-75% B from 40 to 55 min and retain until 58 min then return to initial 20% B in 2 min and maintained for a further 5 min for column equilibrium.

Negative electrospray source was introduced based on preliminary experiment results. The IT-TOF mass conditions were as follows: CDL temperature, 200℃, block heater temperature, 200℃, nebulizing gas (N_2) flow rate, 1.5 L/min, drying gas (N_2) pressure, 0.1 MPa, ion trap pressure, 1.7×10^{-2} Pa, ion accumulated time, 30 ms. Detector voltage was set at -3.5 kV in negative ion electrospray mode. A full scan and automatic multiple stage fragmentation mass spectra were acquired in the range of *m/z* 150–1500 for MS^1, 100–1500 for MS^2, and 50–1500 for MS^3. Argon was used as the collision gas for collision induced dissociation experiments. In order to obtained sufficient fragment ions, the collision energy was set at 50% for MS^2 and 100% for MS^3 respectively according to preliminary experiment. Prior to data acquisition, Trifluroacetaic acid (TFA) sodium solution was used as a standard to calibrate the instrument against the entire mass range (*m/z* 50–5000).

2.4 Peak selection and data processing

It has been found in the preliminary study that the peaks with intensity below 10000 supplied few fragments; therefore, only the peaks detected with intensity over 10000 were selected for further identifications. The chemical formulas for all selected peaks were calculated from the accurate mass using the formula predictor software by setting the parameters as follows: C [0-60], H [0-150], O [0-30], N [0-10], double bond equivalent (DBE) [0-20], and H/C ratio [0-3]. Other elements such as P, S, Cl and Br were not included since they were rarely present in herbal components. The maximum tolerance of mass error was set at 5 ppm. Data acquisition and analysis was performed with LC Solution 3.0 software (Shimadzu, Kyoto, Japan).

2.5 Structure identification

To facilitate structural characterization, the diagnostic ion filtering method was applied based on previous research conducted in our laboratory [9-10]. Briefly, many components in TCMP could be structurally classified into several groups which contained the same carbon skeleton or substructures, thus they may frequently generate the same fragment ions during collision induced dissociation and these fragment ions could be defined as diagnostic fragment ions (DFIs). Once the DFIs has been recognized, it could be used as a prior filtering criterion to screen the candidates in the chemical databases (e.g., Pubchem Compound and Dictionary of Natural Products) according to the predicted formulas, and the compound of a certain group can easily be deduced from the accurate mass distances between quasi-molecular ions and the corresponding serial fragment ions.

3 Results and Discussion

3.1 Peak detection for solvent extraction with different polarity

Figure 1 shows the total ion chromatogram (TIC) of *Yunnan Baiyao* extracted by solvents with distinctive polarity, respectively. The peaks with mass intensity over 10000 were numbered, and those peaks having the same retention time (error limit less than 0.1 min) and accurate molecular weight of precursor ion (error limit less than 5 mDa) were regarded as the same component. In total, 34 components in *Yunnan Baiyao* were detected and different numbers of detected peaks were found in portions extracted with different solvents. Specifically, 25 peaks were detected in the 70% ethanol extracted portion, 26 peaks were found in the n-butanol extracted portion, and only 5 peaks were detected in the di-Ethyl Ether extracted portion. However, those 5 peaks (Peak 30 - Peak 34) were only detected in di-Ethyl Ether extracted portion, indicating that no single extraction solvent can well extract all the components from Yunnan Baiyao. Clearly, the routine use of 70% ethanol for extraction of *Yunnan Baiyao* and other TCMP may easily miss the low polarity components. Thus, in order to obtain a comprehensive chemicalome for qualitative analysis of TCMP, it is highly necessary to use different polarity extraction solvents collaboratively.

3.2 Comparison of integral peak area of precursor ion and fragment ion profile

Usually, the components with higher polarity are eluted earlier on C_{18} reversed-phase column. Thus, as seen in Table 1, according to the relationship between polarity and retention time, all 34 components in *Yunnan Baiyao* can be divided into three segments: segment I,

peak of 1 to 12 (Rt: 3.83-22.31 min) which were deemed as high polarity components presented the maximum integral area of precursor ion in the high polarity extraction solvent portion (70% ethanol); Similarly, segment II (Peak 13 - Peak 29, Rt: 22.82-43.21 min) and segment III (Peak 30 - Peak 34, Rt: 44.23-49.43 min), which included the medium polarity and low polarity components in *Yunnan Baiyao* respectively, both presented the maximal integral area of precursor ion in its corresponding polarity extraction solvent portions (n-butanol for segment II and di-Ethyl Ether for segment III). These results confirmed that high polarity extraction solvent exhibited stronger extraction capability for high polarity components while medium/low polarity extraction solvent is optimal for the extraction of medium/low polarity components. Thus, compared with single extraction solvent, collaboratively using different polarity extraction solvent can efficiently enrich all components from *Yunnan Baiyao* and subsequently elevate target exposure level in MS scan mode.

It is well accepted that precursor ion with higher integral area in MS^1 is apt to generate more fragment ions in the following MS^2 and MS^3. In line with the integral peak area of precursor ion (Table 1), the components in segment I except Peak 11 and Peak 12 generated more fragment ions in 70% ethanol portion compared with other portions, and a similar phenomenon also has been observed for components presented in segment II and segment III. N-butanol and di-Ethyl Ether portion respectively introduced more detailed fragment ions information. e.g., Peak 19 (classified into segment II), its precursor ion at *m/z* 1029.53 $[M-H]^-$ was both detected in 70% ethanol and n-butanol portions, however, only one fragment ion at *m/z* 737.41 in MS^2 was observed in 70% ethanol portion; Oppositely, three fragment ions at

m/z 883.47, 737.41, and 591.35 in MS^2 and two fragment ions at *m/z* 591.35 and 429.29 in MS^3 were observed in the n-butanol portion. These results indicated that combinatorially using different polarity solvent to extract *Yunnan Baiyao* can effectively enrich the fragment ions information.

3.3 Structure characterization

With the advantage of sufficient fragment ions information, a program developed by our laboratory was introduced to rapidly identify the common fragment ions [22]. Components sharing same fragment ions were classified into one group. As a result, 33 out of 34 components were classified into 6 groups (See in Table 2). For group I, the common ions were 475.37 and 391.28, after querying the chemical databases according to the calculated formula, the component with fewest hits was preferentially inferred from the mass difference between fragment ions, e.g., Peak 2 (5 hits on database) was prior identified, the fragment ions $[M\text{-}H\text{-}C_5H_8O_4]^-$ at *m/z* 799.48 and $[M\text{-}H\text{-}C_5H_8O_4\text{-}C_6H_{10}O_5]^-$ at *m/z* 637.43 could be attributed to the successive loss of xylopyranosyl and glucosyl, the common ions $[M\text{-}H\text{-}C_5H_8O_4\text{-}2\times C_6H_{10}O_5]^-$ at *m/z* 475.37 and $[M\text{-}H\text{-}C_5H_8O_4\text{-}2\times C_6H_{10}O_5\text{-}C_6H_{12}]^-$ at *m/z* 391.28 were separately deducted as the aglycone and the aglycone lost a side chain (Figure 2a). Finally, Peak 2 was deduced as Notoginsenoside R_1 and confirmed by comparing chromatography behaviors with its authentic standard. Thus the DFIs of group Ⅰ were determined as *m/z* 475.37 ($C_{30}H_{51}O_4$) corresponding to $[Protopanaxatriol\text{-}H]^-$ and *m/z* 391.28 ($C_{24}H_{39}O_4$) corresponding to $[Protopanaxatriol\text{-}H\text{-}C_6H_{12}]^-$. Based on these DFIs, components in group I could be classified into Protopanaxatriol glycosides. The saccharine moiety could

be rapidly inferred from the mass difference between fragment ions, e.g., the mass difference with 162 Da indicated the loss of glucosyl, and the mass difference with 146 Da possibly indicated the elimination of rhamnosyl. Thus, Peak 3 and Peak 23 could be easily inferred as Ginsenoside Re and Rg_2 respectively. The two pairs of isomers (Peak 4 & Peak 9; Peak 13 & Peak 15) which exerted the same fragment ions were deduced as Ginsenoside Rg_1/Rf and Ginsenoside Rh_1/F_1, respectively. Further, these two pairs of isomers were successfully distinguished by comparing the retention time with corresponding authentic standards. Similarly, for group II, a pair of isomer (Peak 8 & Peak 11) exerted fewest hits during database querying (4 hits on database). By comparing with authentic standard, Peak 11 was prior identified as Ginsenoside Ra_3, the DFIs were determined as *m/z* 459.37 ($C_{30}H_{51}O_3$) corresponding to [Protopanaxadiol-H]$^-$ and *m/z* 375.28 ($C_{24}H_{39}O_3$) corresponding to [Protopanaxadiol-H-C_6H_{12}]$^-$, the characteristic fragmental pathway was shown in Figure 2b and the components in group II were classified into Protopanaxadiol glycosides. For group III, Peak 5 (5 hits on database) was prior identified, the DFIs were determined as *m/z* 593.35 ($C_{33}H_{53}O_9$) corresponding to [furostan-H+$C_6H_{10}O_5$]$^-$ and *m/z* 431.29 ($C_{27}H_{43}O_4$) corresponding to [furostan-H]$^-$ (Figure 2c). The components in group III were deduced as furostan glycosides. For group IV, Peak 21 (9 hits on Database) was prior identified, the DFIs were determined as *m/z* 591.35 ($C_{33}H_{51}O_9$) corresponding to [pennogenin-H+$C_6H_{10}O_5$]$^-$ and *m/z* 429.29 ($C_{27}H_{41}O_4$) corresponding to [pennogenin-H]$^-$ (Figure 2d). The components in group IV were deduced as pennogenin glycosides. For group V, Peak 26 (6 hits on Database) was prior identified as Parissaponin Pb and confirmed by comparing with authentic standard, the DFIs were determined as *m/z* 575.35 ($C_{33}H_{51}O_8$) corresponding to

[diosgenin-H+$C_6H_{10}O_5$]$^-$ and *m/z* 413.29 ($C_{27}H_{41}O_3$) corresponding to [diosgenin-H]$^-$ (Figure 2e). The components in group V were deduced as diosgenin glycosides.

For group VI, the prominent mass differences were 44 Da and/or 28 Da, and it could be inferred that neutral loss of CO_2 and/or CO was the major fragmental pathways. For example, peak 30 yielded fragment ions in MS^2 spectrum at *m/z* 441.34 and 425.34 corresponding to [M- H-CO]$^-$ and [M-H-CO_2]$^-$ (Figure 2f). By comparison with the authentic standards, Peak 30 was identified as gypsogenin, Thus, the common ion *m/z* 441.34 ($C_{29}H_{45}O_3$) was determined as DFIs and according to the fragmental pathway, other components in this group were easily inferred.

For Peak 1, failing to be incorporated into the groups above, eluting at 3.83 min, gave the [M-H]$^-$ ion at *m/z* 175.03 (predicated formula: $C_5H_7N_2O_5$) in MS^1 spectrum. The MS^2 spectrum yielded prominent ions at *m/z* 131.0465 ($C_4H_7N_2O_3$) and *m/z* 87.0592 ($C_3H_7N_2O$) corresponding to [M-H-CO_2]$^-$ and [M-H-2CO_2]$^-$. This peak was identified as Dencichine. In summary, although some isomers couldn't be unambiguously differentiated due to lack of authentic standard, e.g., Peak 14 & Peak 16, using this diagnostic ion filtering strategy, 34 compounds was structurally characterized in a fast and reliable manner, and 21 components were reported in *Yunnan Baiyao* for the first time (Figure 3).

4 Concluding remarks

Efficient sample extraction process was the first key step for qualitative analysis of TCMP. In the present study, collaboratively using extraction solvents with different polarity for sample preparation of TCMP can effectively increase the number of peaks detected and

enrich the fragment ions information with MS technology. Also, a diagnostic ion filtering strategy with LC-IT-TOF/MS was employed for rapid characterization of components from Yunnan Baiyao. A total of 34 components have been successfully identified, out of which, 21 components were reported for the first time. More importantly, the strategy presented here could open perspectives for similar studies on other medicinal herbal prescriptions.

Acknowledgement

This study was supported by National Nature Science Fund (81102881, 30973583, and 30801422), National Key New Drug Creation Special Programme (2009ZX09304-001; 2009ZX09502-004), the Program for New Century Excellent Talents in University (NCET-09-0770), and the Project Program of State Key Laboratory of Natural Medicines, China Pharmaceutical University (No. JKGQ201109).

Conflict of interest statement

The authors declared no conflict of interest.

References

[1] Sun, H., Wu, F., Zhang, A., Wei, W., Han, Y., Wang, X., *J. Sep. Sci.* 2013, 36, 485-491.

[2] Borchers, A. T., Sakai, S., Henderson, G. L., Harkey, M. R., Keen, C. L., Stern, J. S., Terasawa, K., Gershwin, M. E., *J. Ethnopharmacol.* 2000, 73, 1-13.

[3] Wing-Shing, C. D., Koon, C. M., Ng, C. F., Leung, P. C., Fung, K. P., Kar-Sing, P. S., Bik-San, L. C., *J. Ethnopharmacol.* 2012, 143, 859-866.

[4] Wang, X., Zhang, A., Sun, H., *OMICS.* 2012, 16, 414-421.

[5] Wang, Q., Shi, R., Ma, Y. M., Jiang, P., Zhong, J., Cui, H. Y., Liu, P., Liu, C. H., *J. Pharm. Biomed. Anal.* 2013, 77C, 88-93.

[6] Fu, J., Li, X., Lu, H., Liang, Y., *J. Sep. Sci.* 2012, 35, 2940-2948.

[7] Qi, L. W., Wen, X. D., Cao, J., Li, C. Y., Li, P., Yi, L., Wang, Y. X., Cheng, X. L., Ge, X. X., *Rapid Commun. Mass Spectrom.* 2008, 22, 2493-2509.

[8] Zheng, X., Shi, P., Cheng, Y., Qu, H., *J. Chromatogr. A* 2008, 1206, 140-146.

[9] Zheng, C., Hao, H., Wang, X., Wu, X., Wang, G., Sang, G., Liang, Y., Xie, L., Xia, C., Yao, X., *J. Mass Spectrom.* 2009, 44, 230-244.

[10] Hao, H., Cui, N., Wang, G., Xiang, B., Liang, Y., Xu, X., Zhang, H., Yang, J., Zheng, C., Wu, L., Gong, P., Wang, W., *Anal. Chem.* 2008, 80, 8187-8194.

[11] Chen, Q., He, H., Li, P., Zhu, J., Xiong, M., *Biomed. Chromatogr.* in press. DOI: 10.1002/bmc.2847.

[12] Hamed, A. I., Janda, B., Mahalel, U. A., Stochmal, A., Oleszek, W., *Phytochem Anal.* 2012, 23, 613-621.

[13] Li, H. L., Tang, J., Liu, R. H., Lin, M., Wang, B., Lv, Y. F., Huang, H. Q., Zhang, C., Zhang, W. D., *Rapid Commun. Mass Spectrom.* 2007, 21, 869-879.

[14] Zhang, Y., Shi, Q., Shi, P., Zhang, W., Cheng, Y., *Rapid Commun. Mass Spectrom.* 2006, 20, 2328-2342.

[15] Cheng, X. L., Wan, J. Y., Li, P., Qi, L. W., *J. Chromatogr. A* 2011, 1218, 5774-5786.

[16] Xie, T., Liang, Y., Hao, H., A, J., Xie, L., Gong, P., Dai, C., Liu, L., Kang, A., Zheng, X., Wang, G., *J. Chromatogr. A* 2012, 1227, 234-244.

[17] Wu, L. Z., Zhang, X. P., Xu, X. D., Zheng, Q. X., Yang, J. S., Ding, W. L., *J. Pharm. Biomed. Anal.* 2013, 75, 55-63.

[18] Qiu, X., Zhang, J., Huang, Z., Zhu, D., Xu, W., *J. Chromatogr. A* in press. DOI: 10.1016/j.chroma.2012.11.051.

[19] Ladas, E. J., Karlik, J. B., Rooney, D., Taromina, K., Ndao, D. H., Granowetter, L., Kelly, K. M., *Support. Care Cancer* 2012, 20, 3379-3383.

[20] Tang, Z. L., Wang, X., Yi, B., Li, Z. L., Liang, C., Wang, X. X., *Int. J. Oral Maxillofac. Surg.* 2009, 38, 261-266.

[21] Liu, X. X., Wang, L., Chen, X. Q., Deng, X. T., Cao, Y., Wang, Q., *J. Sep. Sci.* 2008, 31, 3834-3846.

[22] Gong, P., Cui, N., Wu, L., Liang, Y., Hao, K., Xu, X., Tang, W., Wang, G., Hao, H., *Anal. Chem.* 2012, 84, 2995-3002.

Figure 1: Total ion chromatograms of YNBY by LC-IT-TOF/MS operated under the negative ionization mode: (A) YNBY extracted by 70% Ethanol and 25 components have been detected; (B) YNBY extracted by n-Butanol and 26 components have been detected; (C) YNBY extracted by Di-Ethyl Ether and 5 components have been detected.

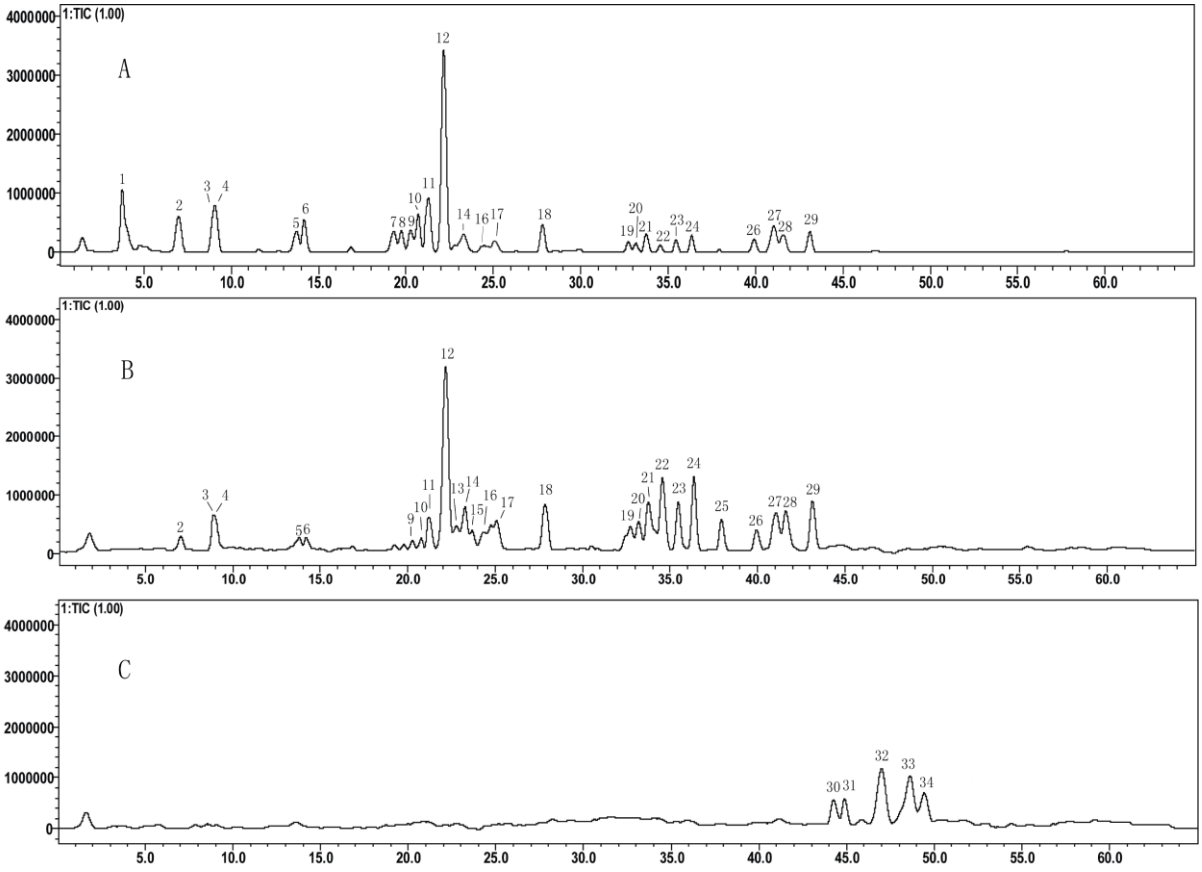

Figure 2: The proposed fragmentation pathways and the structures of diagnostic fragment ions (DFI) for each group.

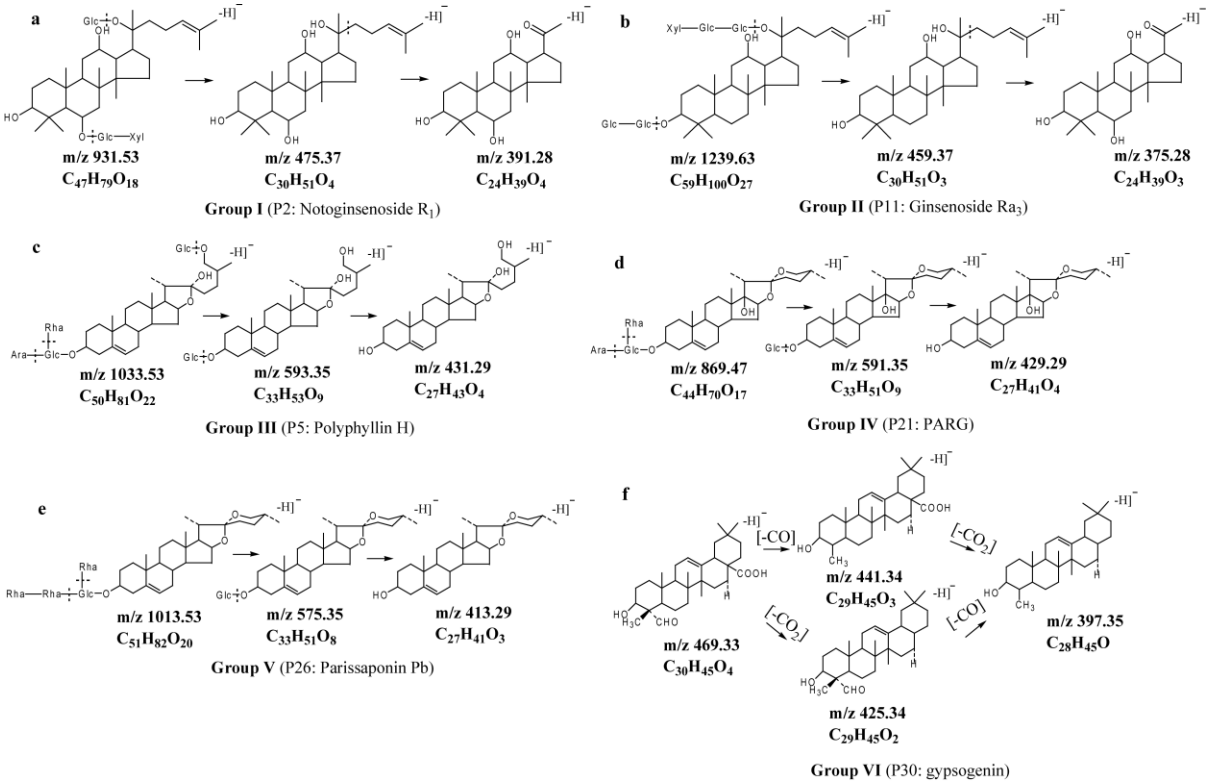

Figure 3: Structural characterization of all detected components in YNBY.

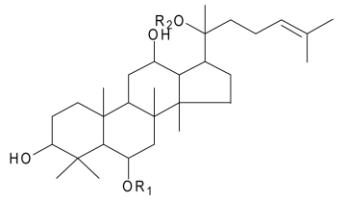

group I

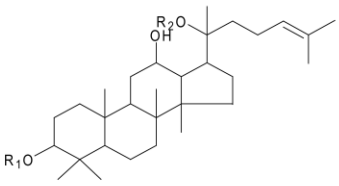

group II

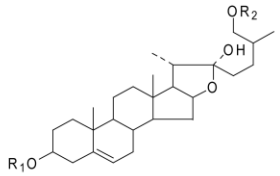

group III

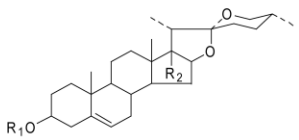

group IV & V

peak no.	R_1	R_2	identification
group I			
2	Xyl-Glc-	Glc-	Notoginsenoside R_1[a]
3	Rha-Glc-	Glc-	Ginsenoside Re
4	Glc-	Glc-	Ginsenoside Rg_1[a]
9	Glc-Glc-	H-	Ginsenoside Rf[a]*
10	Xyl-Glc-	H-	Notoginsenoside R_2*
13	Glc-	H-	Ginsenoside Rh_1[a]*
15	H-	Glc-	Ginsenoside F_1[a]*
23	Rha-Glc-	H-	Ginsenoside Rg_2*
group II			
8	Glc-Glc-	Xyl-Glc-Glc-	Notoginsenoside R_4*
11	Glc-Glc-	Xyl-Glc-Glc-	Ginsenoside Ra_3[a]*
12	Glc-Glc-	Glc-Glc-	Ginsenoside Rb_1
14	Glc-Glc-	Xyl-Ara-Glc-	Ginsenoside Ra_1/Ra_2*
16	Glc-Glc-	Xyl-Ara-Glc-	Ginsenoside Ra_1/Ra_2*
17	Glc-Glc-	Ara-Glc-	Ginsenoside Rc*
18	Glc-Glc-	Glc-	Ginsenoside Rd
24	Glc-	Glc-	Ginsenoside F_2*
25	Glc-Glc-	H-	Ginsenoside Rg_3*
group III			
5	Ara-Glc- | Rha	Glc-	Polyphyllin H*
6	Rha-Glc- | Rha	Glc-	Protogracillin*
7	Rha-Glc-	Glc-	Protobioside*
group IV & V			
19	Rha-Rha-Glc- | Rha	OH-	PRRRG[b]
20	Rha-Glc- | Glc	OH-	PRGG[b]
21	Rha-Glc- | Ara	OH-	PARG[b]
22	Rha-Glc-	OH-	PRG[b]
26	Rha-Rha-Glc- | Rha	H-	Parissaponin Pb[a]
27	Rha-Glc- | Glc	H-	Gracillin
28	Rha-Glc- | Ara	H-	Parissaponin Pa
29	Rha-Glc-	H-	Polyphyllin C*

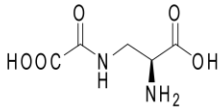

Peak 1: Dencichine

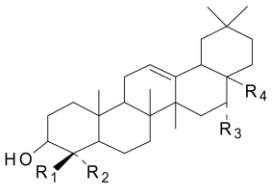

group VI

peak no.	R_1	R_2	R_3	R_4	Identification
group VI					
30	CH_3-	CHO-	H-	COOH-	gypsogenin[a]*
31	CHO-	CH_3-	H-	COOH-	epigypsogein*
32	CH_3-	COOH-	H-	COOH-	gypsogenic acid*
33	CH_3-	CHO-	OH-	COOH-	quillaic acid*
34	CH_3-	CHO-	OH-	$COOCH_3$-	quillaic acid methylate*

[a]: compared with standard subantance; *: reported for first time

PRRRG[b]: Pennogenin-3-O-α-L-Rhamnopyranosyl (1→4)-α-L-Rhamnopyranosyl (1→4)-[α-L-Rhamnopyranosyl (1→2)]-β-D-Glucopyranoside

PRGG[b]: Pennogenin-3-O-α-L-Rhamnopyranosyl (1→2)-[β-D-Glucopyranosyl (1→3)]-β-D-Glucopyranoside

PARG[b]: Pennogenin-3-O-α-L-Rhamnopyranosyl (1→2)-[α-L-Arabinopyranosyl (1→4)]-β-D-Glucopyranoside

PRG[b]: Pennogenin-3-O-α-L-Rhamnopyranosyl (1→2)-β-D-Glucopyranoside

Table 1. Peak areas of precursor ions and MS^n information of detected components from three extracted portions

peak	Rt	precursor Ion	70% ethanol			n-Butanol			di-Ethyl Ether		
no.	(min)	$[M-H]^-$ (*m/z*)	peak area	MS^2 (*m/z*)	MS^3 (*m/z*)	peak area	MS^2 (*m/z*)	MS^3 (*m/z*)	peak area	MS^2 (*m/z*)	MS^3 (*m/z*)
1	3.83	175.03	12536521	131.0465, 87.0562, 59.0617	-	0	-	-	0	-	-
2	7.15	931.53	8125124	799.4843, **637.4319**, 475.3781	475.3777, 391.2850	2017135	799.4841, **637.4315**, 475.3784	475.3772	0	-	-
3	8.93	945.54	821413	799.4839, **783.4889**, **637.4321**, 619.4208, 475.3787	619.4211,475.3775,391.2849	395643	799.4841,783.4886,**637.4325**	475.3778	0	-	-
4	9.12	799.48	10638522	**637.4331**, 475.3792	475.3784, 391.2854	6938483	**637.4329**, 475.3791	475.3782, 391.2850	0	-	-
5	13.61	1033.53	851234	901.4812, 887.4723, 871.4816, **755.4134**	593.3588, 431.2992	159222	755.4127	-	0	-	-
6	14.22	1063.53	1445211	917.4743, **771.4152**, 755.4127	593.3574, 431.2987	162341	771.4158	-	0	-	-
7	19.24	901.47	945151	755.4114, **593.3568**	431.2993	93421	-	-	0	-	-
8	19.73	619.31[a]	797321	1107.5941, 945.5512, **783.4924**, 621.4385	621.4392, 459.3783, 375.2892	93325	-	-	0	-	-
9	20.32	799.48	456837	**637.4325**, 475.3786	475.3782, 391.2849	103251	637.4319	-	0	-	-
10	20.81	769.48	1032631	**637.4331**, 475.3772	475.3779,391.2835	199453	637.4326	-	0	-	-
11	21.33	619.31[a]	5609813	1107.5938, 945.5521, **783.4917**, **621.4377**, 459.3773	621.4365, 459.3768, 375.2886	2465887	945.5513, **783.4925**, **621.4371**, 459.3778	621.4363, 459.3781, 375.2889	0	-	-
12	22.31	553.29[a]	9133650	945.5508, **783.4921**, **621.4381**, **459.3774**, 375.2891	621.4383, 459.3770, 375.2885	8565341	945.5515, **783.4916**, **621.4375**, **459.3785**, 375.2885	621.4374, 459.3775, 375.2894	0	-	-
13	22.82	637.43	83161	-	-	582871	475.3768	391.2842	0	-	-

14	23.35	604.31[a]	408327	945.5516, **783.4918**, 621.4375	621.4374, 459.3782	1658762	945.5521, **783.4924**, 621.4375, 459.3778	621.4365, 459.3791, 375.2896	0	-	-
15	23.82	637.43	45994	-	-	487336	475.3778	391.2851	0	-	-
16	24.34	604.31[a]	144385	783.4922	-	383578	945.5519, **783.4918**, 621.4381	621.4357, 459.3793, 375.2895	0	-	-
17	25.13	1077.58	247438	783.4918, 621.4369	-	869453	945.5524, 915.5348, **783.4928**, **621.4379**	621.4374, 459.3784, 375.2882	0	-	-
18	27.91	945.54	5124512	**783.4921**, 621.4365, 459.3779	-	10856392	**783.4914**, 621.4383, 459.3778, 375.2898	459.3762, 375.2876	0	-	-
19	32.86	1029.53	225458	737.4102	-	852865	883.4708, **737.4112**, 591.3532	591.3541, 429.2935	0	-	-
20	33.22	899.47	233245	737.4114	-	934521	753.4128, **737.4122**	591.3536, 429.2941	0	-	-
21	33.95	869.47	563892	723.4123	-	2163451	737.4135, **723.4136**	591.3528, 429.2930	0	-	-
22	34.54	737.41	201876	-	-	3526425	**591.3518**	429.2937	0	-	-
23	35.53	783.49	314274	637.4328	-	1847356	**637.4325**, 475.3774	475.3776, 391.2843	0	-	-
24	36.42	783.49	203573	621.4375	-	2165841	**621.4371**, 459.3782	459.3774, 375.2882	0	-	-
25	38.04	783.49	16927	-	-	741957	**621.4378**, 459.3788	459.3781, 375.2876	0	-	-
26	40.09	1013.53	213358	721.4159	-	464987	867.4735, **721.4163**, 575.3583	575.3589, 413.2989	0	-	-
27	41.12	883.47	863988	721.4164	-	1145982	737.4153, **721.4157**, 575.3589	575.3592, 413.2978	0	-	-
28	41.73	853.47	566439	721.4152	-	958547	**721.4153**, 707.4148, 575.3574	575.3578, 413.2982	0	-	-
29	43.21	721.41	587423	-	-	1262541	**575.3582**	413.2985	0	-	-

30	44.23	469.33	0	-	-	0	-	-	557428	**441.3437**, 425.3428, 397.3518	397.3523
31	44.95	469.33	0	-	-	0	-	-	613816	**441.3432**, 425.3431, 397.3526	397.3525
32	47.04	485.33	0	-	-	0	-	-	13215362	**441.3428**, 397.3523	397.3519
33	48.82	485.33	0	-	-	0	-	-	10763854	**457.3405**, **441.3421**, 413.3528	413.3516
34	49.43	499.35	0	-	-	0	-	-	688472	**471.3622,** **469.3323,** **441.3429,** **413.3517**	413.3511

[a] types of precursor ions: $[M-2H]^{2-}$

The fragment ions with high response (intensity >10 000) generated in MS^2 which were shown in bold font and underlined were automatically selected for MS^3 fragmentations

Table 2. Diagnostic fragment ions determinations, group classification, predicted formula, and hits of database querying

group	diagnostic fragment ions	peaks of each group	predicted formula (ppm [a])	No. of database hits
I	475.37, 391.28	2, 3, 4, 9, 10, 13, 15, 23	$C_{47}H_{80}O_{18}$ (1.53), $C_{48}H_{82}O_{18}$ (2.41), $C_{42}H_{72}O_{14}$ (1.66), $C_{42}H_{72}O_{14}$ (0.12), $C_{41}H_{70}O_{13}$ (2.83), $C_{36}H_{60}O_{9}$ (-2.21), $C_{36}H_{60}O_{9}$ (-2.17), $C_{42}H_{72}O_{13}$ (0.31)	5, 13, 33, 33, 15, 27, 27, 17
II	459.37, 375.28	8, 11, 12, 14, 16, 17, 18, 24, 25	$C_{59}H_{100}O_{27}$ (-2.31), $C_{59}H_{100}O_{27}$ (-2.39), $C_{54}H_{92}O_{23}$ (2.57), $C_{58}H_{98}O_{26}$ (-0.28), $C_{58}H_{98}O_{26}$ (-0.16), $C_{53}H_{90}O_{22}$ (1.92), $C_{48}H_{82}O_{18}$ (4.21), $C_{42}H_{72}O_{13}$ (0.44), $C_{42}H_{72}O_{13}$ (0.51)	4, 4, 9, 6, 6, 12, 13, 17, 17
III	593.35, 431.29	5, 6, 7	$C_{50}H_{82}O_{22}$ (3.24), $C_{51}H_{84}O_{23}$ (-1.84), $C_{45}H_{74}O_{18}$ (-1.03)	5, 12, 27
IV	591.35, 429.29	19, 20, 21, 22	$C_{51}H_{82}O_{21}$ (1.04), $C_{45}H_{72}O_{18}$ (0.57), $C_{44}H_{70}O_{17}$ (3.63), $C_{39}H_{62}O_{13}$ (1.16)	20, 23, 9, 24
V	575.35, 413.29	26, 27, 28, 29	$C_{51}H_{82}O_{20}$ (1.24), $C_{45}H_{72}O_{17}$ (1.18), $C_{44}H_{70}O_{16}$ (3.35), $C_{39}H_{62}O_{12}$ (-0.38)	6, 23, 18, 15
VI	441.34	30,31,32,33,34	$C_{30}H_{46}O_{4}$ (0.58), $C_{30}H_{46}O_{4}$ (0.67), $C_{30}H_{46}O_{5}$ (1.68), $C_{30}H_{46}O_{5}$ (2.25), $C_{31}H_{48}O_{5}$ (2.19)	116, 116, 95, 95, 38

[a] : differences between the observed precursor ion *m/z* and theoretical *m/z* values